Engineering 45 (2025) 165–173

Contents lists available at ScienceDirect

Engineering

journal homepage: www.elsevier.com/locate/eng

Research
Material Science and Engineering—Article

Highly Efficient and Precise Rare-Earth Elements Separation and Recycling Process in Molten Salt

Hang Hua [a], Kouji Yasuda [b], Yutaro Norikawa [a], Toshiyuki Nohira [a,*]

[a] Institute of Advanced Energy, Kyoto University, Kyoto 611-0011, Japan
[b] Graduate School of Engineering, Kyoto University, Kyoto 606-8501, Japan

ARTICLE INFO

Article history:
Received 21 August 2022
Revised 26 October 2022
Accepted 5 December 2022
Available online 2 September 2024

Keywords:
Neodymium magnet scrap
Rare-earth separation
Dysprosium
Molten salt
Electrochemical formation

ABSTRACT

Owing to the worldwide trend towards carbon neutrality, the number of Dy-containing heat-resistant Nd magnets used for wind power generation and electric vehicles is expected to increase exponentially. However, rare earth (RE) elements (especially Dy) are unevenly distributed globally. Therefore, an environmental-friendly recycling method for RE elements with a highly precise separation of Dy and Nd from end-of-life magnets is required to realize a carbon-neutral society. As an alternative to traditional hydrometallurgical RE separation techniques with a high environmental load, we designed a novel, highly efficient, and precise process for the separation and recycling of RE elements from magnet scrap. As a result, over 90% of the RE elements were efficiently extracted from the magnets using $MgCl_2$ and evaporation loss was selectively suppressed by adding CaF_2. The extracted RE elements were electrolytically separated based on the formation potential differences of the RE alloys. Nd and Dy metals with purities greater than 90% were estimated to be recovered at rates of 96% and 91%, respectively. Almost all the RE in the scraps could be separated and recycled as RE metals, and the byproducts were easily removed. Thus, this process is expected to be used on an industrial scale to realize a carbon-neutral society.

1. Introduction

It is known that rare-earth (RE) magnets are superior to other permanent magnets, such as ferrite and alnico magnets. In particular, Nd magnets exhibit excellent magnetic characteristics and are widely used in mobile phones, wind turbines, and motors for battery electric vehicles (BEVs) and hybrid electric vehicles (HEVs). They are the strongest magnets available on the market with a maximum energy product of 470 $kJ\cdot m^{-3}$ [1]. In addition to the superior magnetic properties of Nd magnets, other advantages include reasonable production costs and high mechanical strength. Despite these promising characteristics, Nd magnets possess a low Curie temperature of 310 °C [2]. Therefore, to maintain their superior magnetic properties at high temperatures, other RE elements, such as Tb and Dy, must be added to Nd magnets. The high heat resistance of these magnets is achieved by replacing a fraction of the Nd atoms with Tb or Dy atoms at the grain boundaries of the $Nd_2Fe_{14}B$ phase; however, this step decreases the magnetic moment (the resulting magnets are called heat-resistant Nd magnets) [3,4]. Dy is often added to Nd magnets for economic reasons.

Because BEVs/HEVs emit lower amounts of carbon dioxide than conventional gasoline-driven vehicles, they are expected to become more popular because of their contribution to carbon neutrality. Consequently, the production of BEVs/HEVs is expected to increase rapidly in the near future, increasing the demand for Nd and Dy. However, heavy RE elements, such as Dy, are unevenly distributed in limited countries [5]. Although heavy RE mines are also found in some countries, they are difficult to handle because of radioactive tailings from Th and U in RE ores.

Recycling RE from RE-containing scrap is a sustainable method for their production in countries without RE resources that desire to decrease their environmental loads. Currently, RE elements accumulated in home appliances, such as air conditioners contain-

---

[*] Corresponding author.
E-mail address: nohira.toshiyuki.8r@kyoto-u.ac.jp (T. Nohira).

https://doi.org/10.1016/j.eng.2022.12.013

ing Nd magnets, are expected to become alternative RE resources [6]. In 2020, approximately 160 000 t of Nd-sintered magnets and 12 000 t of bonded magnets were sold worldwide [7]. Furthermore, the amount of Nd magnet scraps will increase with the increasing popularity of BEVs/HEVs in the foreseeable future, necessitating the development of a feasible technique for recycling RE elements from Nd magnet scraps. Currently, only a small fraction of RE elements is recycled from in-process scraps produced at magnet manufacturing plants, which are usually recovered by hydrometallurgical methods [8–10]. During the recycling of scraps of heat-resistant Nd magnets, the separation of Nd and Dy metals is a critical step because a mixture of Nd and Dy is inadequate as a raw material for heat-resistant Nd magnets. However, owing to its various disadvantages, such as the presence of multiple stages, high energy consumption, and high environmental impact, this process has not been widely adopted and is only used in magnet manufacturing plants. The large amount of Nd magnet scrap generated daily is either disposed as garbage or accumulated in urban mines.

Recently, several new RE-recycling methods have been proposed. Two of these methods involve RE separation based on differences in the vapor pressures of various RE complexes. The first method involves a reaction with aluminum chloride vapor at high temperatures to synthesize complexes containing RE elements with high vapor pressures [11–15]. The second method separates RE components using the difference between the vapor pressures of chlorides or iodides of different valences [16,17]. Although these two methods are simpler than the hydrometallurgical process with fewer steps and the separation factor of Nd and Sm is relatively high, the separation factor of Nd and Dy is not ideal. Several selective extraction methods that use metals, oxides, chlorides, and fluorides as extraction agents at high temperatures have been developed [18–29]. Although many of these techniques can successfully separate RE elements from non-RE elements, the high-precision separation of individual RE elements has not yet been implemented. A molten salt electrolysis method based on a bipolar alloy diaphragm with a high separation efficiency for individual RE elements has been proposed previously [30–33]. It has been experimentally confirmed that Dy can be selectively separated from molten LiCl–KCl containing both Dy and Nd by precisely controlling its electrolysis potential [31]. Because of the high formation rate of the $DyNi_2$ alloy, high-precision and efficient RE separation can be realized. Various advantages such as fewer steps, high purity of the produced RE elements, and high Dy/Nd separation ratio have been discussed in the above-mentioned studies; however, the durability and strength of the $DyNi_2$ alloy are insufficient to perform long-term electrolysis.

Herein, a novel RE recycling process is proposed to separate and recover individual RE elements from Nd magnet scraps; this is called the selective extraction–evaporation–electrolysis (SEEE) process because it includes three main steps: ① selective extraction, ② selective evaporation, and ③ selective electrolysis (Fig. 1). In this method, RE are extracted from Nd magnet scraps using a $CaCl_2$-based molten salt. After removing the remaining extraction agent and byproduct, Nd and Dy are electrochemically separated using a Ni electrode. The principles of each step of the recycling process are described in detail in Section 3. We tested $CaCl_2$–CaF_2–$MgCl_2$ as a molten salt, and the obtained results characterized the main process steps, including the extraction of RE elements from commercial heat-resistant Nd magnets, removal of Mg components by vacuum evaporation, and electrochemical separation of Nd and Dy. Based on the study findings, the RE contained in Nd magnet scrap can be efficiently recovered as a high-purity metal, which will reduce the risk of RE supply for countries lacking RE reserves.

2. Materials and methods

2.1. Extraction of RE and evaporation of Mg

Commercial heat-resistant Nd magnets (NE206; diameter, 10 mm; thickness, 2 mm; Niroku Seisakusho Co., Ltd., Japan) were used as simulated magnet scraps. Before the experiment, the magnets were demagnetized by heat treatment at 773 K for 1 h in vacuum. The magnet composition was determined by inductively coupled plasma atomic emission spectroscopy (ICP–AES; SPECTROBLUE, AMETEK, Inc., USA) after dissolution in nitric acid (Wako 1st Grade, FUJIFILM Wako Pure Chemical Corp., Japan) and included 0.9 weight percent (wt%) B, 1.0 wt% Cu, 66.5 wt% Fe, 2.3 wt% Ni, 20.3 wt% Nd, 6.6 wt% Pr, and 2.4 wt% Dy. Ni and Cu were detected because they were used as coating materials. Each magnet was broken in half using two pliers to expose the Nd magnet surface, and a $CaCl_2$ (99%; Kojundo Chemical Laboratory Co., Ltd., Japan) and $MgCl_2$ (99.9%; Kojundo Chemical Laboratory Co., Ltd.) powder mixture was added. To prevent the evaporation of the extracted RE halides, 2, 4, and 6 mole percent (mol%) CaF_2 (99.9%; Kojundo Chemical Laboratory Co., Ltd.) were added to the mixture. The amount of molten salt was selected to ensure that the RE concentration was 2 mol% when all the RE content in the magnet was extracted. All the reagents were added to a graphite crucible (IG-110; inner diameter, 49 mm; height, 150 mm; Sanko Co., Ltd., Japan), dehydrated in a vacuum oven at 453 K for 72 h, and placed at the bottom of a stainless-steel vessel inside an airtight Kanthal container for further dehydration under vacuum at 773 K for 24 h. After dehydration, the Kanthal container was replenished with Ar gas, and the temperature was raised to 1123 K and maintained for 20 h to complete the RE extraction process. After 20 h, the temperature was increased to 1273 K, and the reaction mixture was kept under vacuum for 3 h to remove the unreacted $MgCl_2$ and Mg byproducts. The magnet and molten salt were cooled to room temperature and recovered by crushing in a crucible. The magnet was then washed with water and dried in a vacuum oven at 453 K. One piece of the magnet was embedded in acrylic resin, polished to expose the cross-section, and analyzed using scanning electron microscopy (SEM; Phenom Pro Generation 5, Thermo Fisher Scientific Inc., USA) and energy-dispersive X-ray spectroscopy (EDX; SE1200–8001, Thermo Fisher Scientific Inc.). Another piece of the magnet was dissolved in nitric acid and analyzed by ICP–AES. A portion of the recovered salt that did not contain CaF_2 was ground in a ceramic mortar and subjected to ICP–AES analysis using the same method. The salt fraction containing CaF_2 was analyzed by Techno Science Corp. (Japan). X-ray diffraction (XRD; Ultima IV, Rigaku Corp., Japan) was performed on the magnets before and after extraction using Cu Kα radiation ($\lambda = 0.15418$ nm) at a voltage of 40 kV and current of 40 mA. The compounds collected from the low-temperature part of the container top after RE extraction were also analyzed using XRD.

2.2. Electrolysis separation of Dy and Nd

The preparation of the molten salts and experimental apparatus have been described previously [34,35]. Additional details are provided below. The magnet used in the RE extraction experiment contained Nd, Dy, and Pr as RE elements. Because the chemical properties of Pr and Nd are similar, electrolysis separation experiments were conducted in molten salts containing only Nd and Dy for simplicity. Based on the results of the RE extraction and Mg evaporation experiments performed in this study, and the RE electrolysis separation conducted in our previous work [36], two

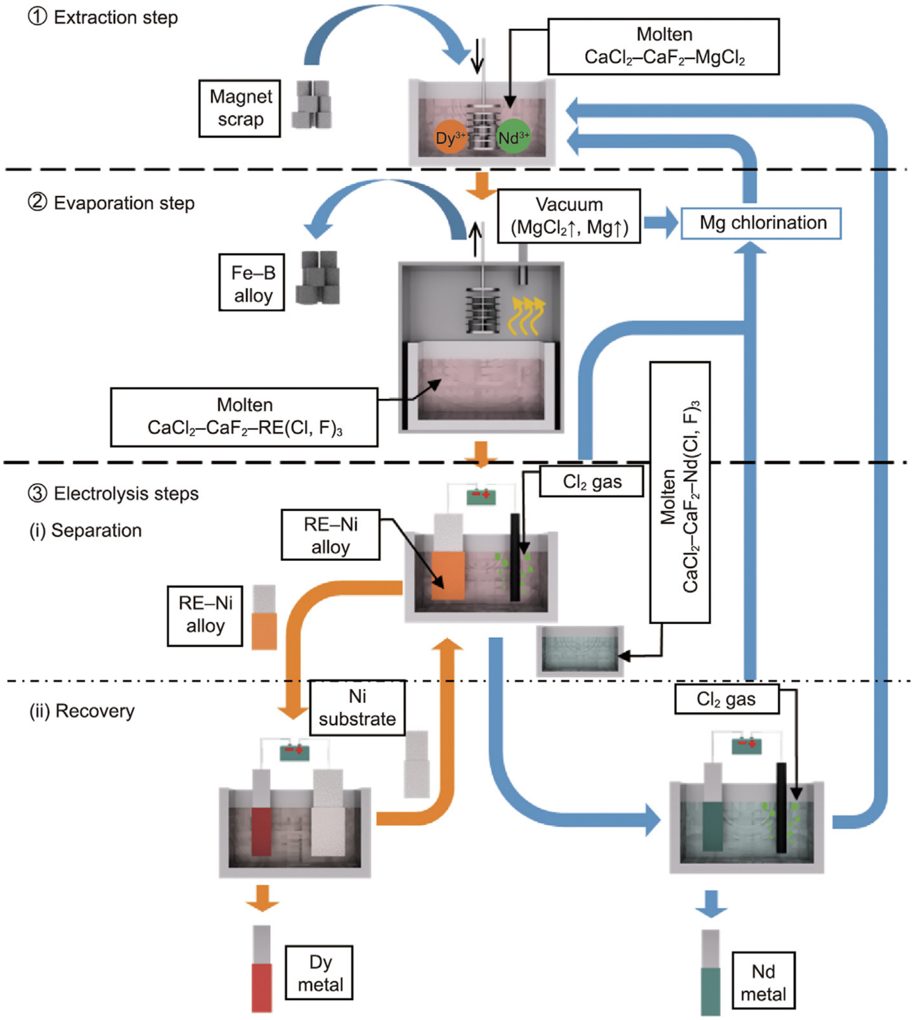

Fig. 1. Schematic of the SEEE process.

molten salt systems with the same elemental molar ratio, F/(Nd + Dy) ratio of 6, were prepared. The first molten salt was $CaCl_2$–CaF_2 (6.00 mol%)–$NdCl_3$ (1.83 mol%)–$DyCl_3$ (0.17 mol%). Its Dy/Nd ratio was 0.09, which is similar to that of the commercial heat-resistant Nd magnet used in the RE extraction experiment. The second molten salt was $CaCl_2$–CaF_2 (9.00 mol%)–$NdCl_3$ (2.00 mol%)–$DyCl_3$ (1.00 mol%). Its Dy/Nd ratio was set to 0.5, which is close to that of the Nd magnets used in the motors of BEVs/HEVs. $NdCl_3$ (99.9%) and $DyCl_3$ (99.9%) were purchased from Kojundo Chemical Laboratory Co., Ltd. The samples fabricated in these two systems were analyzed using XRD and SEM/EDX.

3. Results and discussion

3.1. Process design

A conceptual diagram of the SEEE process is shown in Fig. 1. First, the Nd magnet scraps were immersed in a molten $CaCl_2$–CaF_2 system containing $MgCl_2$ for RE element extraction. According to the Ellingham diagrams of chlorides and fluorides depicted in Figs. 2(a) and (b) [37], the standard Gibbs formation energies of Mg chloride and fluoride are more negative than those of Cu, Ni, Fe, B, and Al, and more positive than those of Nd, Dy, and Ca. Fe, B, Nd, and Dy are the main components of heat-resistant Nd magnets, and Cu, Ni, and Al are typically used as coating materials to prevent magnet oxidation. These results indicate that $MgCl_2$ and MgF_2 do not react with Cu, Ni, Fe, B, or Al but interact with Nd and Dy; therefore, only RE elements are extracted into molten $CaCl_2$–CaF_2 after the extraction step. Unlike the process developed by Shirayama and Okabe [29] in which pure $MgCl_2$ was used as the extraction agent, $CaCl_2$ was the main component of the molten salt in the process proposed in this study, and a small amount of $MgCl_2$ was added for RE extraction. In addition, $CaCl_2$ and CaF_2 do not react with any of the metals listed in the two diagrams. After the RE extraction using Mg^{2+}, Cu, Ni, Fe, B, and Al were separated by removing the solid phase. Finally, Nd and Dy were extracted from the melt as chlorides or fluorides, respectively.

After the RE extraction step, the liquid phase was composed of Mg metal and chlorides and fluorides of Mg, Nd, Dy, and Ca. Fig. 2(c) shows the calculated vapor pressures of the compounds [37]. The solid lines indicate the values calculated from the thermodynamic parameters of the liquid phase, and the broken lines denote the values extrapolated from the thermodynamic parameters of the liquid phase at high temperatures. The vapor pressures of Mg and $MgCl_2$ are equal to 8.6×10^{-2} and 2.4×10^{-3} atm (1 atm = 101 325 Pa) at 1123 K, respectively, which are much higher than those of the other compounds. Therefore, Mg and $MgCl_2$ can be easily removed under vacuum. As $NdCl_3$ and $DyCl_3$ also have relatively high vapor pressures, they may partially

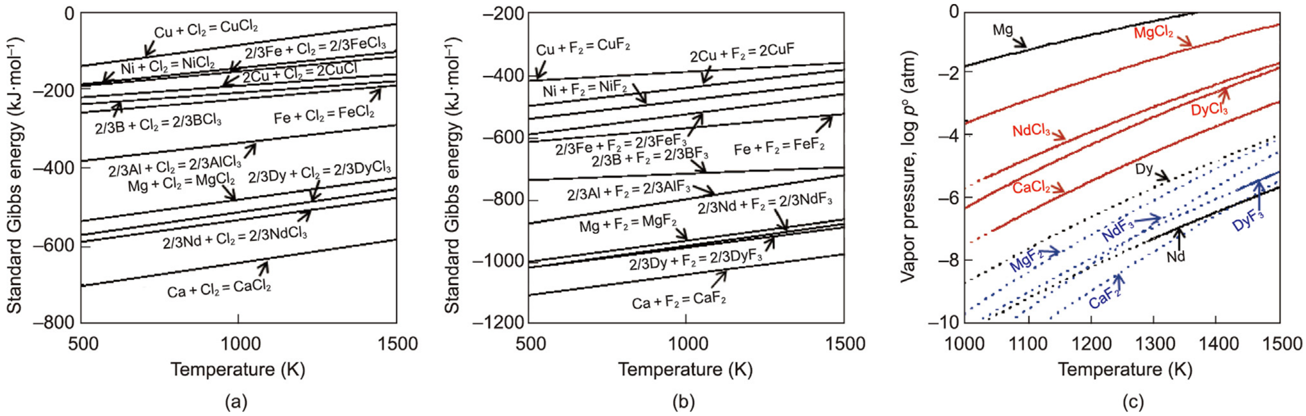

Fig. 2. (a, b) Standard Gibbs formation energies of several (a) chlorides and (b) fluorides. The thermodynamic parameters for the temperatures below the melting points were determined by the extrapolation of the liquid state data obtained at high temperatures to study the stability of molten salts. (c) Vapor pressures of various compounds that are likely formed during the evaporation step. The solid lines indicate the liquid states, and the broken lines represent the extrapolations of the liquid state data obtained at high temperatures. 1 atm = 101 325 Pa.

evaporate with Mg and $MgCl_2$. Thus, CaF_2 was initially added to the melt to fluorinate the Nd and Dy compounds and decrease their vapor pressures. The evaporated Mg and $MgCl_2$ were reused as extraction agents after chlorination.

Electrolysis separation of the obtained melt was performed using Ni metal and carbon as the cathode and anode, respectively. The Cl_2 gas generated at the carbon anode was used to chlorinate the Mg byproduct in the previous step. Unlike the process reported by Oishi et al. [30], in which an RE–Ni alloy was used as a bipolar electrode, Ni metal served as the cathode to form the RE–Ni alloy in the present study. A specific RE–Ni alloy with a high Dy/Nd ratio was obtained by controlling the electrolysis potential. The produced alloy was transported to another melt for use as the anode, where the RE elements were selectively and anodically dissolved. Finally, the separated RE were electrodeposited on the cathode surface. After the RE were fully dissolved, the remaining Ni metal was reused as a cathode in the previous step. The molten salt obtained after Dy separation was regenerated by electrodeposition of metallic Nd on the cathode surface. The regenerated molten salt and chlorinated Mg were reused in the RE extraction step. The experimental methodology for each step is described in Appendix A.

3.2. RE extraction and Mg evaporation

3.2.1. Analysis of Nd magnets

Figs. 3(a)–(c) show the photograph, XRD pattern, and cross-sectional SEM image of a commercial heat-resistant Nd magnet. According to the ICP–AES and EDX data, the metallic luster layer covering the magnet surface consisted of a Cu–Ni alloy. Because Cu and Ni do not react with $MgCl_2$, owing to their thermodynamic properties, the magnet was broken in half to expose the Nd magnet phase prior to the RE extraction experiment. The broken Nd magnet was powdered and analyzed by XRD, wherein $Nd_2Fe_{14}B$ was observed as the main phase. The cross-sectional SEM image reveals that the Nd magnet alloy is dense and consists of Fe- and RE-rich phases. The dark part is an Fe-rich phase with a Nd + Pr concentration of 10–15 atomic percent (at%), which represents the $Nd_2Fe_{14}B$ phase, and the bright part is the RE-rich phase with a Nd + Pr concentration higher than 90 at%. As the energies of the characteristic Dy and Fe X-ray peaks were very similar, the Dy concentration could not be accurately determined using EDX.

After the extraction of the RE components from the magnets with different $MgCl_2$ concentrations and evaporation of the Mg byproduct, the magnets were analyzed using the same methods. Figs. 3(d)–(f) show a photograph, XRD pattern, and cross-sectional SEM image of the Nd magnet obtained after RE extraction with 3 mol% $MgCl_2$ in molten $CaCl_2$ at 1123 K for 20 h and Mg vacuum evaporation at 1273 K for 3 h. A comparison of Figs. 3(a) and (d) suggests that the magnet volume changed very little after the RE extraction and Mg evaporation. The XRD pattern of the magnet after the RE extraction corresponded to that of the Fe phase, indicating that almost all the RE species were extracted from the magnet. Although the presence of B was not confirmed by XRD, the B component was expected to remain in the solid phase in the form of an Fe–B(s) alloy produced via reaction (1) during RE extraction [29], as follows:

$$RE_2Fe_{14}B(s) + 3MgCl_2(l) \rightarrow 2RECl_3(l) + Fe-B(s) + 3Mg(l) \tag{1}$$

Cross-sectional SEM images confirmed the presence of multiple pores and a decrease in the RE-rich phase content after extraction. The average Nd and Pr concentrations determined using EDX were less than 0.1 at%. The concentration of Dy atoms could not be accurately measured for the above-mentioned reason. As the Nd and Pr concentrations were close to 0, it was concluded that almost all RE species were extracted from the magnet.

The extraction ratios of the RE elements were estimated from the changes in their concentrations in the magnet after the reaction and were calculated from the results of the ICP–AES analysis (Table 1). Because Fe does not react with $MgCl_2$, the concentrations of the RE elements are listed as mass ratios with respect to the Fe content. In the initial magnet, the concentration of Dy, Nd, and Pr atoms were 36.0, 304.4, and 99.0 mg per gram of Fe (g-Fe), respectively. According to reaction (1), the stoichiometric amount of Mg^{2+} consumed during RE extraction was 1.5 times larger than that of RE. Because the amount of RE elements in the magnet corresponded to 2 mol% of the molten salt, 3 mol% of Mg^{2+} ion was required to completely extract these elements. For samples 1, 2, and 3, the added amounts of $MgCl_2$ were 1, 2, and 5 times larger than the stoichiometric amount required for 100% extraction of RE elements, respectively.

After the initial addition of $MgCl_2$ (sample 1), the concentrations of Dy, Nd, and Pr were 2.5, 8.2, and 2.2 mg·g-Fe^{-1}, which corresponded to the Dy, Nd, and Pr extraction ratios of 93%, 97%, and 98%, respectively. Here, the RE extraction reaction (1) is considered in the simplified form of reaction (2) for thermodynamic considerations:

$$2RE(s) + 3MgCl_2(l) = 2RECl_3(l) + 3Mg(l) \tag{2}$$

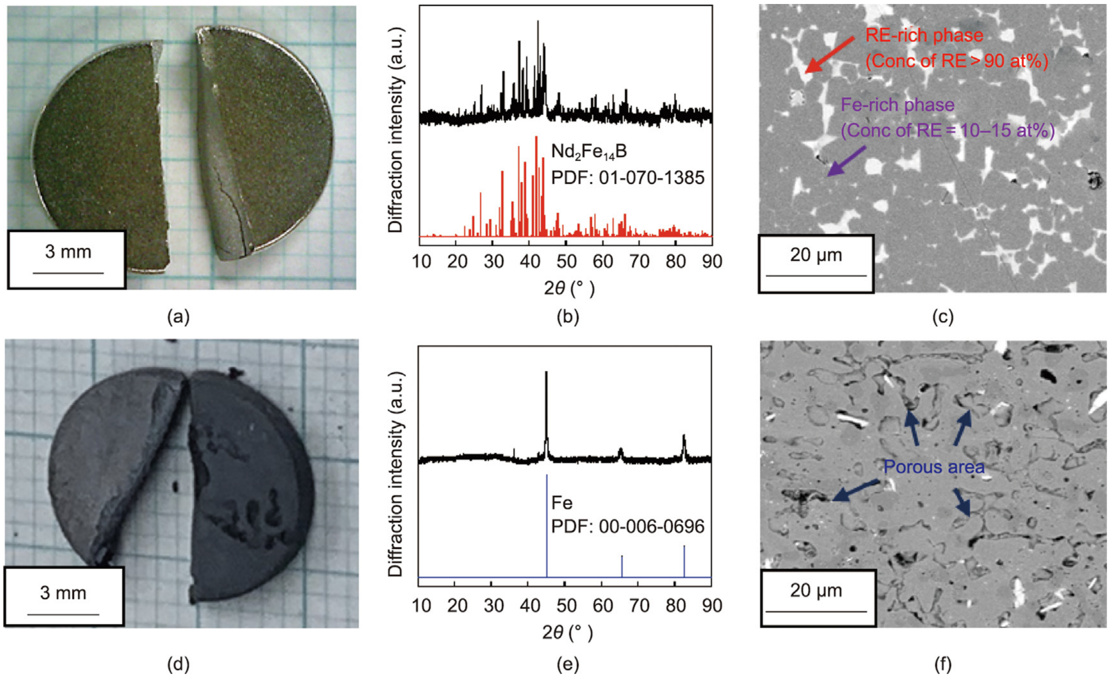

Fig. 3. (a) Photograph, (b) XRD pattern, and (c) cross-sectional SEM image of the commercial heat-resistant Nd magnet obtained before the RE extraction. (d) Photograph, (e) XRD pattern, and (f) cross-sectional SEM image of the commercial heat-resistant Nd magnet obtained after the RE extraction by 3 mol% $MgCl_2$ in molten $CaCl_2$ at 1123 K for 20 h and Mg evaporation in vacuum at 1273 K for 3 h. PDF: powder diffraction file; Conc: concentration.

Table 1
Concentrations of RE elements in the Nd magnets measured before and after the RE extraction at 1123 K for 20 h and Mg evaporation by vacuum at 1273 K for 3 h in molten $CaCl_2$–CaF_2–$MgCl_2$ (Nos. 1–6).

Sample No.	Concentration of added salts (mol%)		Concentration in Nd magnets (mg·g-Fe^{-1})			Extraction ratio (%)		
	$MgCl_2$	CaF_2	Dy	Nd	Pr	Dy	Nd	Pr
Initial magnet	–	–	36.0	304.4	99.0	–	–	–
1	3	0	2.5	8.2	2.2	93	97	98
2	6	0	1.3	4.2	0.6	96	99	99
3	15	0	1.5	4.6	0.6	96	99	99
4	6	2	2.3	7.2	1.7	94	98	98
5	6	4	3.0	8.5	2.4	92	97	98
6	6	6	2.1	6.5	1.6	93	98	98

The standard Gibbs energies of reaction (2) determined for RE of Dy, Nd, and Pr are equal to −70.1, −135.5, and −164.9 kJ·mol^{-1} at 1123 K, respectively [37]. In the experiment of sample 1, RE and $MgCl_2$ were present in stoichiometric amounts prior to reaction (2). The activities of $MgCl_2$ and $RECl_3$ at equilibrium after the reaction were calculated for their standard states corresponding to pure liquids. The RE and Mg activities were assumed to be unity, and the initial $MgCl_2$ and $RECl_3$ were equal to 0.03 and 0, respectively. The activity coefficients of $MgCl_2$ and $RECl_3$ were assumed to be unity. The activities of $DyCl_3$, $NdCl_3$, and $PrCl_3$ obtained after reaction (2) reached equilibrium were 0.0165, 0.0196, and 0.0199, respectively. The RE element content in the magnet was 2 mol% of the molten salt, the activity of $RECl_3$ was equal to 0.02 after their extraction. The calculated extraction ratios of Dy, Nd, and Pr were 82.5%, 98.0%, and 99.5%, respectively. The calculated extraction ratios of Nd and Pr were almost consistent with the experimental values obtained for sample 1; however, the actual extraction ratio of Dy exceeded the calculated value owing to the slightly different activity coefficients in this system (especially that of $DyCl_3$). To verify the RE-extraction limit, experiments involving the addition of larger $MgCl_2$ amounts were performed. When the amount of $MgCl_2$ was doubled (sample 2), the extraction ratios of Dy, Nd, and Pr increased slightly to 96%, 99%, and 99%, respectively. Because the extraction ratios of RE elements remained almost unchanged after increasing the $MgCl_2$ amount by a factor of 5 (sample 3), the RE extraction limit was reached after increasing the $MgCl_2$ content by a factor of 2.

To suppress the evaporation of RE compounds, CaF_2 was also added to the molten salt system to fluorinate the RE elements and decrease their vapor pressures. The influence of CaF_2 addition on RE extraction was investigated for samples 2 and 4–6 containing different amounts of CaF_2 (0, 2, 4, and 6 mol%). Here, 6 mol% of CaF_2 is the stoichiometric amount of F^- required for the octahedral coordination of all RE ions in this system. According to the obtained results, the extraction ratios of Dy, Nd, and Pr slightly decreased after CaF_2 addition but remained large and close to 100%. Therefore, the influence of CaF_2 addition remains negligible when the F^- molar concentration exceeds the RE concentration by a factor of 6 or less.

The ICP–AES data obtained for the original and treated magnets (Table 1) were used to determine the RE extraction parameters. However, they did not show whether the analyzed components remained in the system or were volatilized after the reaction. Hence, ICP–AES analysis of the remaining salts must be performed to evaluate their evaporation behaviors. In particular, $MgCl_2$ traces in the molten salt should be avoided because the electrodeposition of metallic Mg can preferentially occur prior to the electrochemical formation of RE–Ni alloys during electrolysis.

3.2.2. Molten salt analysis and evaporation behavior

The influence of the addition of F^- ions on the evaporation behavior of each component was examined in detail by the ICP–AES analyses of the remaining salts in the experiments of samples 2 and 4–6. The amounts of Dy, Nd, Pr, and Mg in the salts were determined from the ICP–AES data. The evaporation ratios of RE (R_{RE}) and Mg (R_{Mg}) were calculated using Eqs. (3) and (4), respectively:

$$R_{RE} = \left(1 - \frac{W_{RE,salt}}{W_{RE,ext}}\right) \times 100\% \tag{3}$$

$$R_{Mg} = \left(1 - \frac{W_{Mg,salt}}{W_{Mg,ini}}\right) \times 100\% \tag{4}$$

where $W_{RE,salt}$ and $W_{Mg,salt}$ are the masses of RE and Mg present in the remaining molten salts after evaporation, respectively; $W_{RE,ext}$ is the mass of RE extracted from the magnet which can be calculated from the values listed in Table 1; and $W_{Mg,ini}$ is the mass of Mg contained in the initially added $MgCl_2$. Fig. 4 shows the evaporation ratios of Dy, Nd, Pr, and Mg from molten $CaCl_2$–CaF_2 (0–6 mol%)–$MgCl_2$ (6 mol%) obtained after the RE extraction at 1123 K for 20 h and Mg evaporation at 1273 K for 3 h. Without CaF_2 addition, the evaporation ratios of Dy, Nd, Pr, and Mg were equal to 90%, 77%, 73%, and 94%, respectively, and the evaporated species included $DyCl_3$, $NdCl_3$, $PrCl_3$, Mg, and $MgCl_2$. Mg was separated from the other evaporated compounds and collected from the low-temperature part of the container top after RE extraction (Fig. S1 in Appendix A). Although the Mg component was almost completely removed, the loss of RE was relatively high. Upon increasing the CaF_2 concentration, the evaporation ratios of Dy, Nd, and Pr were effectively reduced, whereas those of Mg remained almost constant. At a CaF_2 concentration of 6 mol%, the values obtained for Dy, Nd, Pr, and Mg were 32%, 22%, 5%, and 99%, respectively.

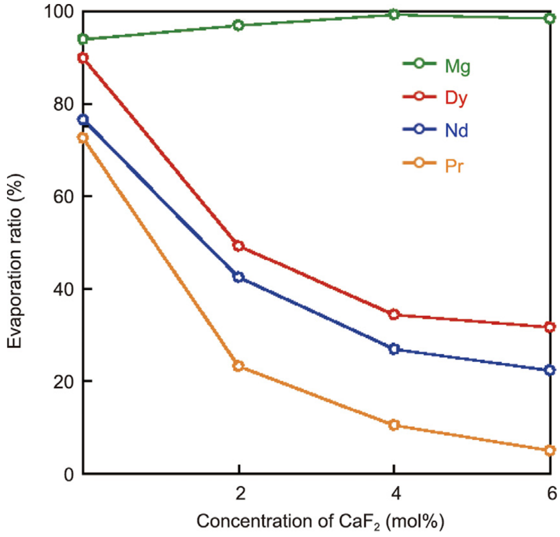

Fig. 4. Evaporation ratios of Dy, Nd, Pr, and Mg from molten $CaCl_2$–CaF_2 (0–6 mol%)–$MgCl_2$ (6 mol%) obtained after the RE extraction at 1123 K for 20 h and Mg evaporation at 1273 K for 3 h.

The observed suppression of RE evaporation can be explained by the formation of low vapor pressure stable octahedral F^--coordinated RE ions DyF_6^{3-}, NdF_6^{3-}, and PrF_6^{3-} as follows:

$$RECl_3(l) + 3CaF_2(l) = REF_6^{3-} + 3Ca^{2+} + 3Cl^- \tag{5}$$

Further suppression of RE evaporation may be achieved by varying the amount of added CaF_2, the evaporation temperature, the evaporation time, or the degree of vacuum. Meanwhile, the evaporation of the Mg species occurred actively because of the presence of high-vapor-pressure $MgCl_2$ when reaction (6) was at equilibrium:

$$MgCl_2(l) + CaF_2(l) = MgF_2(l) + CaCl_2(l) \tag{6}$$

Although the standard Gibbs energy of reaction (6) is −51.0 kJ•mol^{-1} at 1123 K [37], the reaction equilibrium is shifted to the left because of the continuous evaporation and removal of $MgCl_2$.

3.3. Electrolysis separation of Dy and Nd

First, RE separation from magnets with low Dy/Nd ratios was investigated by preparing a molten $CaCl_2$–CaF_2 (6.00 mol%)–$NdCl_3$ (1.83 mol%)–$DyCl_3$ (0.17 mol%) system, whose Dy/Nd molar ratio (0.09) was similar to that of the commercial heat-resistant Nd magnet. Several samples were fabricated by potentiostatic electrolysis with Ni electrodes in the voltage range of 0.40–0.60 V (vs Ca^{2+}/Ca) for 30 min at 1123 K. A cross-sectional SEM image with the EDX analysis results and the XRD pattern of the sample obtained at 0.50 V are shown in Figs. 5(a) and (b), respectively. They show that an RE–Ni alloy layer was formed on the Ni electrode surface. Its formation rate, calculated by dividing the thickness of the alloy layer by the electrolysis time, was 47 μm•h^{-1}. The concentrations of the alloy layer components determined using EDX were 20.2 at% Dy, 10.9 at% Nd, and 68.9 at% Ni. The molar ratio of (Dy + Nd)/Ni was 31.1:68.9, which is close to the molar ratio of $RENi_2$. The XRD profiles confirmed that the alloy layer consisted of $RENi_2$ species. The calculated Dy/Nd ratio was 1.9, which is approximately 21 times higher than the initial Dy/Nd ratio of the molten salt system.

$$f_{enrich} = \frac{x_{Dy,alloy}/x_{Nd,alloy}}{x_{Dy,salt}/x_{Nd,salt}} \tag{7}$$

where f_{enrich} is the enrichment factor for electrolysis; $x_{Dy,alloy}$ and $x_{Dy,salt}$ are molar concentrations of Dy in the alloy and molten salt, respectively; and $x_{Nd,alloy}$ and $x_{Nd,salt}$ are the molar concentrations of Nd in the alloy and molten salt, respectively. The samples obtained at other potentials were analyzed using the same method. Figs. 5(c) and (d) show the potential dependence of the formation rate of RE–Ni alloys, RE concentration, and Dy/Nd ratio in RE–Ni alloys. The obtained Dy + Nd concentrations suggested that $RENi_5$ was formed at 0.60 V and $RENi_3$ at 0.55 V. Although the Dy/Nd ratios at these potentials exceed that of the alloy obtained at 0.50 V, the corresponding alloy formation rates are only 11 and 16 μm•h^{-1}, respectively. Meanwhile, the alloy formation rates obtained at 0.45 and 0.40 V are relatively high (113 and 155 μm•h^{-1}), but the corresponding Dy/Nd ratios are only 0.3 and 0.2, respectively. Considering the formation rate of 47 μm•h^{-1} and Dy/Nd ratio of 1.9, 0.50 V appears to be a suitable potential for Dy enrichment in this system. Although an enrichment factor of approximately 21 was achieved using this method, the Dy/Nd ratio of 1.9 was too low and did not meet high-precision Dy separation requirements. In our previous study, it was found that the alloy formation rate for a highly efficient and precise process should exceed 50 μm•h^{-1} and that the Dy/Nd ratio should be larger than 9 [36].

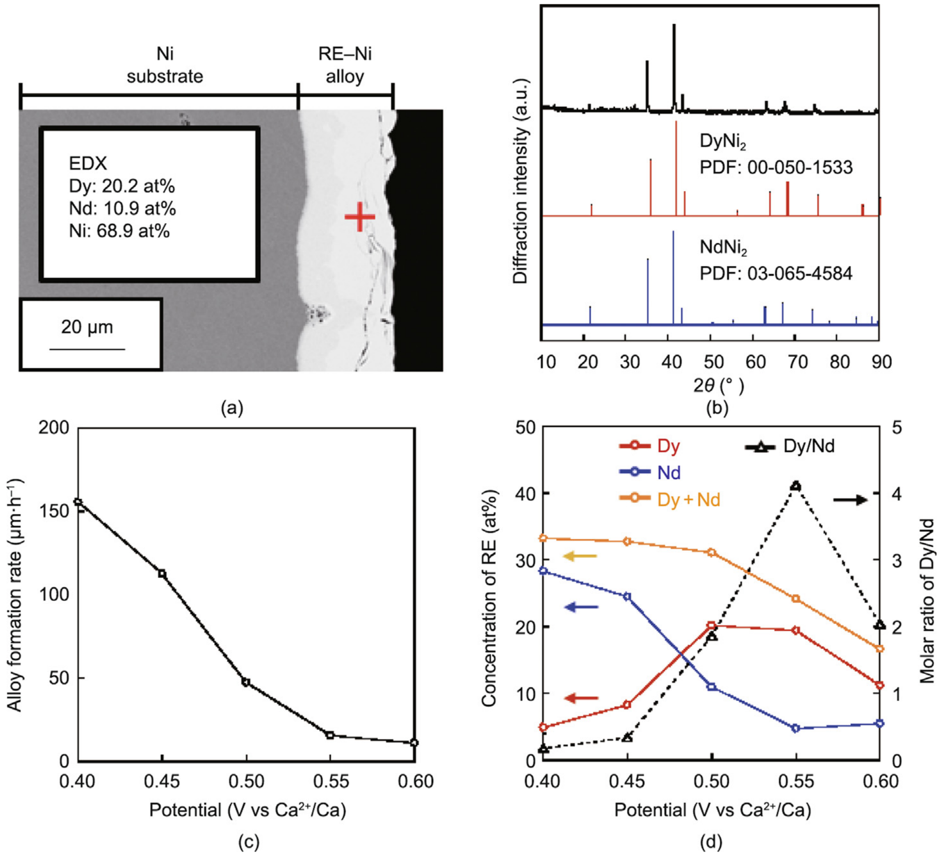

Fig. 5. (a) Cross-sectional SEM image with EDX analysis results and (b) XRD pattern of the sample obtained by the potentiostatic electrolysis with a Ni electrode at a potential of 0.50 V. (c, d) Potential dependences of the (c) RE–Ni alloy formation rate and (d) concentrations of RE elements and Dy/Nd ratio in the RE–Ni alloys. The samples were obtained by the potentiostatic electrolysis with Ni electrodes at various potentials and temperature of 1123 K for 30 min in a molten $CaCl_2$–CaF_2 (6.00 mol%)–$NdCl_3$ (1.83 mol%)–$DyCl_3$ (0.17 mol%) system.

Next, RE separation from the magnets used in the motors of BEVs/HEVs was investigated in molten $CaCl_2$–CaF_2 (9.00 mol%)–$NdCl_3$ (2.00 mol%)–$DyCl_3$ (1.00 mol%) system. Similar to the previous experiments, several samples were prepared by potentiostatic electrolysis with Ni electrodes at 0.40–0.60 V for 30 min at 1123 K. Fig. S2 in Appendix A shows the cross-sectional SEM image with EDX analysis results (Fig. S2(a)) and the XRD pattern of the sample obtained at 0.60 V (Fig. S2(b)). The calculated alloy formation rate was 65 μm·h^{-1}, and the compositions of the alloy layer components determined by EDX were 29.3 at% Dy, 0.7 at% Nd, and 70.0 at% Ni. Both alloy composition and XRD data confirmed the formation of $RENi_2$. The Dy/Nd ratio of 42 obtained for the alloy was 84 times higher than that obtained for the molten salt system (Eq. (7)). Because both the alloy formation rate and Dy/Nd separation ratio for the sample prepared at 0.60 V are relatively high, Dy can be selectively separated with high efficiency and precision under these conditions. The analysis results for the samples prepared at other potentials are shown in Fig. S2. They show that the $RENi_2$ alloy was formed at 0.60 V, and that the highest Dy/Nd ratio was achieved at this potential. Compared with the latter system, the $RENi_2$ alloy was produced at a higher positive potential. As the concentration of the RE component increased, the activity of RE^{3+} also increased, shifting the formation potential of the RE–Ni alloy to positive values. The formation of the $RENi_2$ alloy at 0.60 V was mainly because of the higher Dy concentration in the system. As discussed in our previous study, high Dy/Nd ratios can be obtained at potentials corresponding to different Nd–Ni and Dy–Ni alloy formation rates [36]. Because the alloy formation potential of Dy–Ni was positively shifted in this system, the difference in the alloy formation rates between Nd–Ni and Dy–Ni was larger than that observed for the last system, resulting in a higher Dy/Nd ratio. The Dy/Nd ratios of the samples electrolyzed at 0.55, 0.50, and 0.45 V were above 20, which also met the high-precision Dy separation requirement. Furthermore, the alloy formation rates at these potentials (108, 119, and 196 μm·h^{-1}, respectively) were higher than those at 0.60 V. According to these results, Dy can be separated from the Nd magnets used in BEV/HEV motors with high efficiency and precision.

3.4. SEEE process capability

Finally, the capabilities of the SEEE process were examined. As described above, the purity of the reusable Dy metal should exceed 90%; therefore, the $x_{\mathrm{Dy,alloy}}/x_{\mathrm{Nd,alloy}}$ value must exceed 9. As $x_{\mathrm{Dy,salt}}/x_{\mathrm{Nd,salt}}$ content decreased during electrolysis, it was necessary to consider the lowest limit of $x_{\mathrm{Dy,salt}}/x_{\mathrm{Nd,salt}}$ to obtain a target $x_{\mathrm{Dy,alloy}}/x_{\mathrm{Nd,alloy}}$ of 9. Table 2 summarizes the highest $x_{\mathrm{Dy,alloy}}/x_{\mathrm{Nd,alloy}}$ values obtained for the different molten $CaCl_2$–CaF_2–$NdCl_3$–$DyCl_3$ systems described in the previous section and in our previous study [36]. As mentioned earlier, molten salt with $x_{\mathrm{Dy,salt}}/x_{\mathrm{Nd,salt}} = 0.5$ can be obtained after RE extraction from the Nd magnet scraps used in BEV/HEV motors. Although the highest $x_{\mathrm{Dy,alloy}}/x_{\mathrm{Nd,alloy}}$ value achieved for this system was 42, the $x_{\mathrm{Dy,alloy}}/x_{\mathrm{Nd,alloy}}$ value decreased with decreasing $x_{\mathrm{Dy,salt}}/x_{\mathrm{Nd,salt}}$. As shown in Table 2, the $x_{\mathrm{Dy,alloy}}/x_{\mathrm{Nd,alloy}}$ of 9 was obtained for the molten salt with $x_{\mathrm{Dy,salt}}/x_{\mathrm{Nd,salt}}$ between 0.09 and 0.50. Within this range, it is reasonable to assume that an $x_{\mathrm{Dy,salt}}/x_{\mathrm{Nd,salt}}$ of 0.20 can yield an $x_{\mathrm{Dy,alloy}}/x_{\mathrm{Nd,alloy}}$ of 9. Because the initial $x_{\mathrm{Dy,salt}}/x_{\mathrm{Nd,salt}}$ is

Table 2
Highest Dy/Nd ratios and the corresponding Dy alloy enrichment factors obtained for the molten $CaCl_2$–CaF_2–$NdCl_3$–$DyCl_3$ (F/(Nd + Dy) ratio of 6) salts with different Dy/Nd ratios at 1123 K.

Molten system No.	Concentration of salts composition (mol%)				$x_{Dy,salt}/x_{Nd,salt}$	$x_{Dy,alloy}/x_{Nd,alloy}$	Potential (V vs Ca^{2+}/Ca)	f_{enrich}
	$CaCl_2$	CaF_2	$NdCl_3$	$DyCl_3$				
1	92.0	6.00	1.83	0.17	0.09	4.1	0.55	46
2	88.0	9.00	2.00	1.00	0.50	42.0	0.60	84
3	92.0	6.00	1.00	1.00	1.00	45.0	0.60	45

0.50, approximately 40% of the Dy remains in the molten salt with $x_{Dy,salt}/x_{Nd,salt} = 0.20$, which can be considered to be recovered as another alloy. The Dy/Nd ratio of the magnet scrap is 0.5; hence, if an alloy with an $x_{Dy,alloy}/x_{Nd,alloy}$ of 0.50, or higher, is produced, it can be processed together with the scrap. Table 2 shows that the $x_{Dy,alloy}/x_{Nd,alloy}$ of 0.50 is obtained for a molten salt with an $x_{Dy,salt}/x_{Nd,salt}$ value of less than 0.09. Thus, it can be concluded that the lowest limit of $x_{Dy,salt}/x_{Nd,salt}$ equal to 0.05 can be used to obtain an $x_{Dy,alloy}/x_{Nd,alloy}$ of 0.5.

The recovery rates and purities of the recovered Dy and Nd products were estimated. Fig. 6 shows the changes in $x_{Dy,salt}/x_{Nd,salt}$ and $x_{Dy,alloy}/x_{Nd,alloy}$ during the SEEE process. The final products were Dy metal with $x_{Dy,metal}/x_{Nd,metal} > 9$ (where $x_{Dy,metal}$ and $x_{Nd,metal}$ are molar concentrations of Dy and Nd in the final product, respectively), and Nd metal with $x_{Dy,metal}/x_{Nd,metal} = 0.05$. In separation step, Dy contained in the molten salt with $x_{Dy,salt}/x_{Nd,salt} = 0.50$ was recovered as the RE–Ni alloy with $x_{Dy,alloy}/x_{Nd,alloy} > 9$ until $x_{Dy,salt}/x_{Nd,salt}$ reached 0.20. Furthermore, 61% of Dy and 3% of Nd in the raw material were present in the alloy. In recovery step for Dy, the alloy was used to prepare a Dy metal product with a purity of over 90%, which satisfied the requirements for the manufacture of heat-resistant Nd magnets. To recover the Dy remaining in the molten salt after the separation step, the RE–Ni alloy with $x_{Dy,alloy}/x_{Nd,alloy}$ (> 0.5) was prepared until the $x_{Dy,salt}/x_{Nd,salt}$ value reached 0.05. Here, 33% of Dy and 33% of Nd in the raw material were present in the recycled alloy. The Dy and Nd species present in this alloy were selectively extracted from the starting molten salt together with Nd magnet scraps. In recovery step for Nd, the Nd contained in the molten salt with $x_{Dy,salt}/x_{Nd,salt} = 0.05$ was recovered as the Nd metal product with a purity of 95%. Here, 6% of the Dy and 64% of the Nd in the raw material were present in the Nd metal. Because 33% of Dy and Nd were recycled in the extraction step and Dy losses occurred only because of Nd metal contamination, the calculated recovery rate of Dy was 91%. For the same reason, the calculated Nd recovery rate was 96%. It is noteworthy that unrecovered Dy and Nd are present in the Nd and Dy metals, respectively; therefore, they are not lost during magnet production.

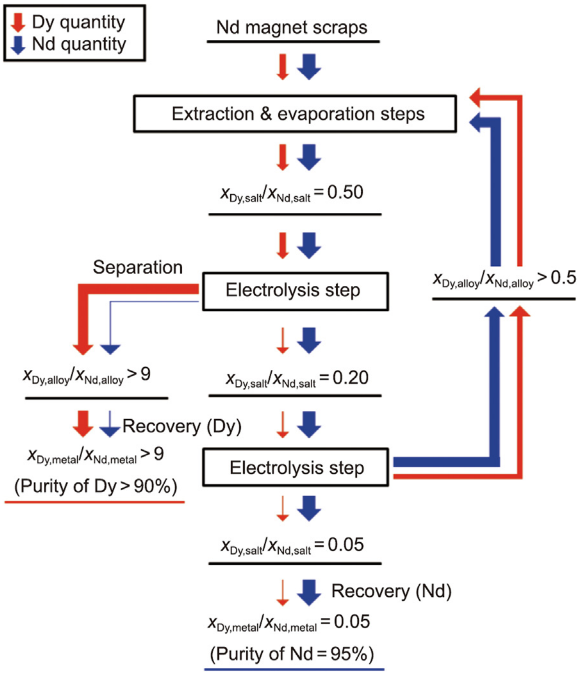

Fig. 6. Dy/Nd ratio changes in the salt, alloy, and metal observed during the SEEE process. The red arrows indicate the Dy amounts, and the blue arrows denote the Nd amounts.

We previously calculated the current efficiency of the $DyNi_2$ alloy formation in a similar molten salt [34]. When a 0.1 mm thick Ni substrate was electrolyzed at 0.5 V versus Ca^{2+}/Ca for 60 min, the Ni substrate was completely alloyed. The calculated current efficiency was 66.6%, even though the alloying reaction should have been completed before the end of electrolysis. In our previous study [36], fully alloyed $DyNi_2$ was formed within 30 min under the same conditions. In this case, the current efficiency is expected to be approximately 20% higher than 66.6%. In this process, the Ni electrode does not need to be fully alloyed. Therefore, the current efficiency of the proposed process should be higher than 85%, satisfying the requirements for efficient processing presented in Ref. [36].

4. Conclusions

In this study, a novel RE separation and recycling process called the SEEE process is proposed. The capability of the SEEE process for recycling REs from Nd magnets used in BEV/HEV motors was estimated by analyzing the Dy/Nd separation data obtained for molten salts with different Dy/Nd ratios. The final Dy product was recovered as Dy metal with a purity of over 90% and a recovery rate of 91%, whereas 96% of the Nd was recovered as Nd metal with a purity of 95%. These results indicate that both Nd and Dy can be recovered as high-purity RE metals at sufficiently high recovery rates, confirming the high processing capability of the SEEE process. This environmental-friendly process for recycling REs from magnets used in BEVs and HEVs is highly significant, given the expected rapid spread of BEVs and HEVs toward achieving carbon neutrality. In addition, this process can be used not only for RE recycling from magnets but also for the reprocessing of nuclear fuels. Although the SEEE process needs to be investigated in technical detail, this study has proven its effectiveness.

Acknowledgments

This work was partially supported by a Grant-in-Aid from the Japan Society for the Promotion of Science (JSPS) Fellows (19J20301).

Compliance with ethics guidelines

Hang Hua, Kouji Yasuda, Yutaro Norikawa, and Toshiyuki Nohira declare that they have no conflict of interest or financial conflicts to disclose.

Appendix A. Supplementary data

Supplementary data to this article can be found online at https://doi.org/10.1016/j.eng.2022.12.013.

References

[1] Jones N. Materials science: the pull of stronger magnets. Nature 2011;472 (7341):22–3.
[2] Coey JMD. Permanent magnet applications. J Magn Magn Mater 2002;248 (3):441–56.
[3] Hirosawa S, Matsuura Y, Yamamoto H, Fujimura S, Sagawa M, Yamauchi H. Magnetization and magnetic anisotropy of $R_2Fe_{14}B$ measured on single crystals. J Appl Phys 1986;59(3):873–9.
[4] Sagawa M, Hirosawa S, Yamamoto H, Fujimura S, Matsuura Y. Nd–Fe–B permanent magnet materials. Jpn J Appl Phys 1987;26(6R):785–800.
[5] US Geological Survey. Mineral commodity summaries 2021. Reston: US Geological Survey; 2021.
[6] Shiratori T, Nakamura T. Concept of artificial mineral deposit—a proposal for employing the concept of "reserve to stock". Shigen-to-Sozai 2006;122(6–7):325–9. Japanese.
[7] Kramer D. US government acts to reduce dependence on China for rare-earth magnets. Phys Today 2021;74(2):20–4.
[8] Xiao W, Pan D, Niu Z, Fan Y, Wu S, Wu W. Opportunities and challenges of high-pressure ion exchange chromatography for nuclide separation and enrichment. Chin Chem Lett 2022;33(7):3413–21.
[9] Xiao J, Li B, Qiang R, Qiu H, Chen J. Highly selective adsorption of rare earth elements by honeycomb-shaped covalent organic frameworks synthesized in deep eutectic solvents. Environ Res 2022;214:113977.
[10] Chen Z, Li Z, Chen J, Kallem P, Banat F, Qiu H. Recent advances in selective separation technologies of rare earth elements: a review. J Environ Chem Eng 2022;10(1):107104.
[11] Adachi G, Murase K, Shinozaki K, Machida K. Mutual separation characteristics for lanthanoid elements via gas phase complexes with alkaline chlorides. Chem Lett 1992;21(4):511–4.
[12] Murase K, Shinozaki K, Hirashima Y, Machida K, Adachi G. Rare earth separation using a chemical vapor transport process mediated by vapor complexes of the $LnCl_3$–$AlCl_3$ system. J Alloys Compd 1993;198(1–2):31–8.
[13] Murase K, Machida K, Adachi G. Recovery of rare metals from scrap of rare earth intermetallic material by chemical vapor transport. J Alloys Compd 1995;217(2):218–25.
[14] Murase K, Ozaki T, Machida K, Adachi G. Extraction and mutual separation of rare earths from concentrates and crude oxides using chemical vapor transport. J Alloys Compd 1996;233(1–2):96–106.
[15] Ozaki T, Jiang J, Murase K, Machida K, Adachi G. Mutual separation characteristics for the yttrium and lanthanides with chemical vapor transport process mediated by metal chloride gaseous complexes. J Alloys Compd 1998;265(1–2):125–31.
[16] Uda T, Jacob KT, Hirasawa M. Technique for enhanced rare earth separation. Science 2000;289(5488):2326–9.
[17] Uda T, Komarov S, Hirasawa M. Dry separation for rare earth by vacuum distillation of di and triiodide mixture. Mater Trans 2001;42(8):1813–9.
[18] Xu Y, Chumbley LS, Laabs FC. Liquid metal extraction of Nd from NdFeB magnet scrap. J Mater Res 2000;15(11):2296–304.
[19] Uda T. Recovery of rare earths from magnet sludge by $FeCl_2$. Mater Trans 2002;43(1):55–62.
[20] Okabe TH, Takeda O, Fukuda K, Umetsu Y. Direct extraction and recovery of neodymium metal from magnet scrap. Mater Trans 2003;44(4):798–801.
[21] Saito T, Sato H, Ozawa S, Yu J, Motegi T. The extraction of Nd from waste Nd–Fe–B alloys by the glass slag method. J Alloys Compd 2003;353(1–2):189–93.
[22] Takeda O, Okabe TH, Umetsu Y. Phase equilibrium of the system Ag–Fe–Nd, and Nd extraction from magnet scraps using molten silver. J Alloys Compd 2004;379(1–2):305–13.
[23] Itoh M, Masuda M, Suzuki S, Machida KI. Recycling of rare earth sintered magnets as isotropic bonded magnets by melt-spinning. J Alloys Compd 2004;374(1–2):393–6.
[24] Takeda O, Okabe TH, Umetsu Y. Recovery of neodymium from a mixture of magnet scrap and other scrap. J Alloys Compd 2006;408–412:387–90.
[25] Itoh M, Miura K, Machida K. Novel rare earth recovery process on Nd–Fe–B magnet scrap by selective chlorination using NH_4Cl. J Alloys Compd 2009;477 (1–2):484–7.
[26] Takeda O, Nakano K, Sato Y. Recycling of rare earth magnet waste by removing rare earth oxide with molten fluoride. Mater Trans 2014;55(2):334–41.
[27] Chae HJ, Kim YD, Kim BS, Kim JG, Kim TS. Experimental investigation of diffusion behavior between molten Mg and Nd–Fe–B magnets. J Alloys Compd 2014;586(Suppl 1):S143–9.
[28] Akahori T, Miyamoto Y, Saeki T, Okamoto M, Okabe TH. Optimum conditions for extracting rare earth metals from waste magnets by using molten magnesium. J Alloys Compd 2017;703:337–43.
[29] Shirayama S, Okabe TH. Selective extraction and recovery of Nd and Dy from Nd–Fe–B magnet scrap by utilizing molten $MgCl_2$. Metall Mater Trans B 2018;49(3):1067–77.
[30] Oishi T, Konishi H, Nohira T, Tanaka M, Usui T. Separation and recovery of rare earth metals by molten salt electrolysis using alloy diaphragm. Kagaku Kogaku Ronbunshu 2010;36(4):299–303. Japanese.
[31] Konishi H, Ono H, Nohira T, Oishi T. Separation of Dy and Nd (La) using molten salt and an alloy diaphragm. ECS Trans 2013;50(11):463–72.
[32] Nohira T, Kobayashi S, Kondo K, Yasuda K, Hagiwara R, Oishi T, et al. Electrochemical formation of RE–Ni (RE = Pr, Nd, Dy) alloys in molten halides. ECS Trans 2013;50(11):473–82.
[33] Yasuda K, Kondo K, Kobayashi S, Nohira T, Hagiwara R. Selective formation of rare-earth–nickel alloys via electrochemical reactions in NaCl–KCl molten salt. J Electrochem Soc 2016;163(5):D140–5.
[34] Hua H, Yasuda K, Konishi H, Nohira T. Electrochemical formation of Dy–Ni alloys in molten $CaCl_2$–$DyCl_3$. J Electrochem Soc 2020;167(14):142504.
[35] Hua H, Yasuda K, Konishi H, Nohira T. Electrochemical formation of Nd–Ni alloys in molten $CaCl_2$–$NdCl_3$. J Electrochem Soc 2021;168(3):032506.
[36] Hua H, Yasuda K, Nohira T. Highly efficient and precise electrolysis separation of dysprosium from neodymium for magnet scrap recycling in molten salt. ACS Sustain Chem Eng 2022;10(28):9225–31.
[37] HSC Chemistry®. Version 9 [software]. Pori: Outotec Information Center; 2015.